Update on EHO Modeling with NIMROD

J R King, S E Kruger

Tech-X Corporation

APS-DPP 2013

Tokamak operation with edge harmonic oscillations (EHO) provides access to a quiescent H-mode regime [Burrell 2012].

- EHO is characterized by a small toroidal mode number (n~1-5) perturbation localized to the magnetic separatrix.
- Particle transport is enhanced leading to steady-state pedestal profiles.
- Access to the EHO operation regime requires control of the flow profile.
- The aim of this work is to ascertain the role of the flow shear.
- In particular, experimental observations indicate that the ExB flow shear is a key component in the generation of EHO [Garofalo 2011].

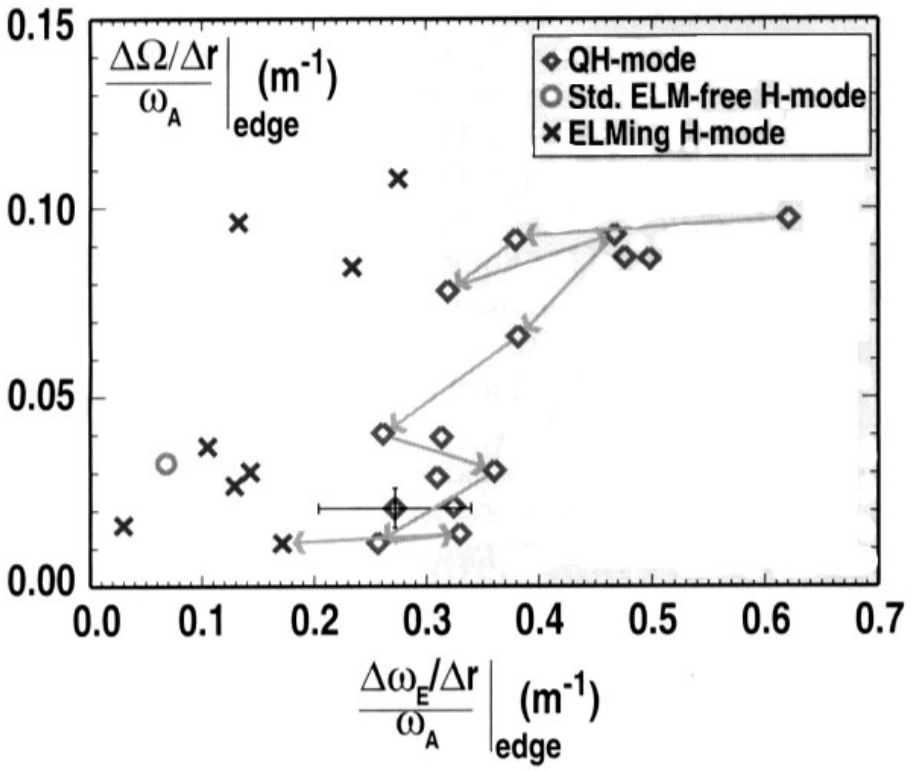

The physical mechanisms of EHO are not fully understood.

- Linear MHD calculations suggest EHO may be a saturated kink-peeling mode partially driven by flow-profile shear [Snyder 2007].
- It is hypothesized that the saturated mode drives sufficient particle and thermal transport to maintain steady state pedestal profiles.
- Our intent is to investigate the nonlinear physics – although our initial results are linear.

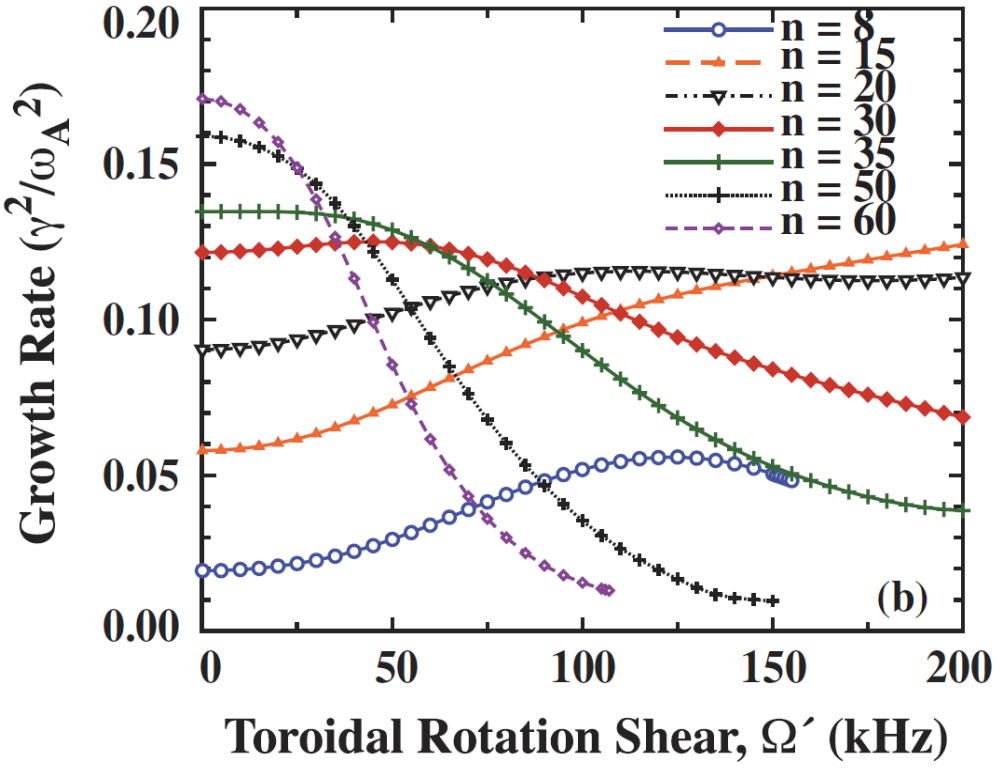

ELITE results from Snyder 2007

Why is NIMROD a suitable code for modeling EHO?

- Experimental observations show EHO is a low-n perturbation and thus global computations are necessary.
- In addition to the capability to model of flow-profile effects, NIMROD also retains important two-fluid and FLR terms.
  - Two-fluid effects are predicted to enhance the growth rate at intermediate wavenumbers and cut it off at large wavenumbers though diamagnetic effects [Hastie, Ramos, Porcelli 2003].
- Even if the high wavenumber modes are stabilized by two-fluid effects, they may be driven nonlinearly. Nonlinear modeling of EHO saturation requires resolution of a large toroidal mode spectrum.
- NIMROD is capable of modeling a realistic x-point geometry.

However, previous work encountered challenges.

- These cases have a relatively high q_{95} (6-7).
- The poloidal-resolution weak scaling for these cases was limited by the amount of system memory (RAM) available.
- NIMROD cases with an ideal-like MHD model at this limited resolution did not agree ELITE computations.

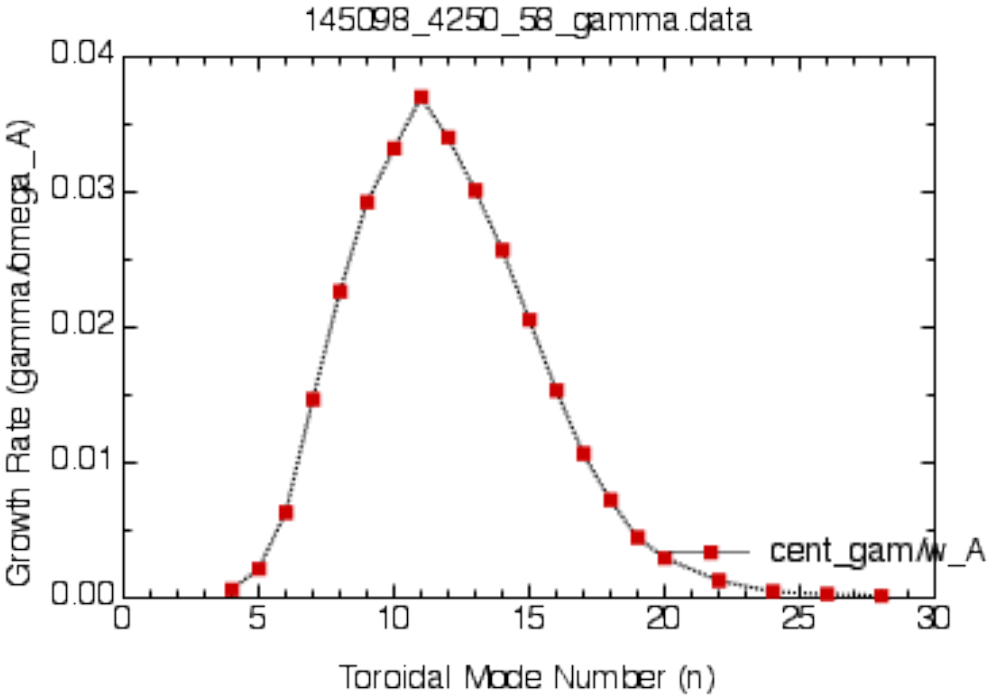

ELITE results courtesy

Phil Snyder

Recent improvements to the NIMROD code enable these EHO computations.

1) Better meshing and projection of the equilibrium onto the NIMROD mesh.
2) Better memory management allows for higher resolution runs that enable the Meudas benchmark.
3) Stabilization techniques for numerical interchange modes at the limit of resolution [C Sovinec earlier talk].

Computations need more resolution along the separatrix near the x-point.

- Our original meshing algorithm produces a flux aligned within the separatrix, and the resolution is limited in expanded-flux regions such as the x-point.
- By abandoning the mesh alignment to the flux in these expanded-flux regions, we achieve better resolution in the separatrix.
- Additionally, more accurate projections onto the NIMROD mesh of magnetic fields and currents are done by using the native finite-element framework to solve from the flux function and F and apply divergence cleaning.

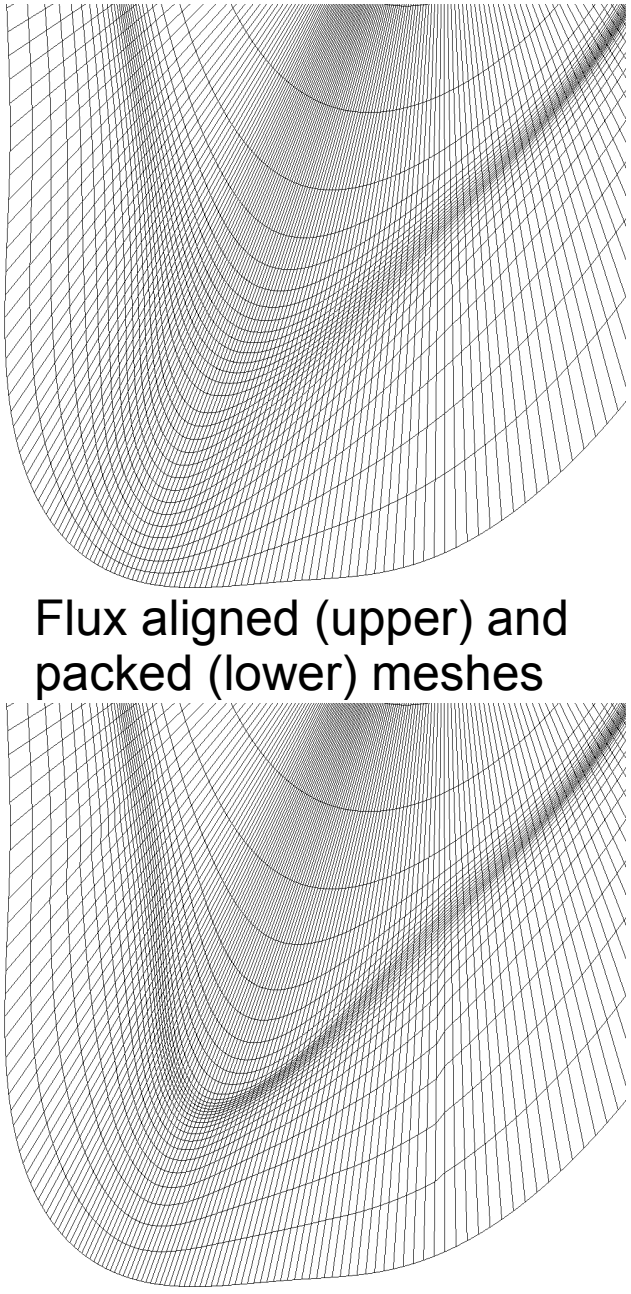

Flux aligned (upper) and packed (lower) meshes

We have a new routine (dsta) that improves the memory efficiency during the export of NIMROD's sparse matrix to external solvers.

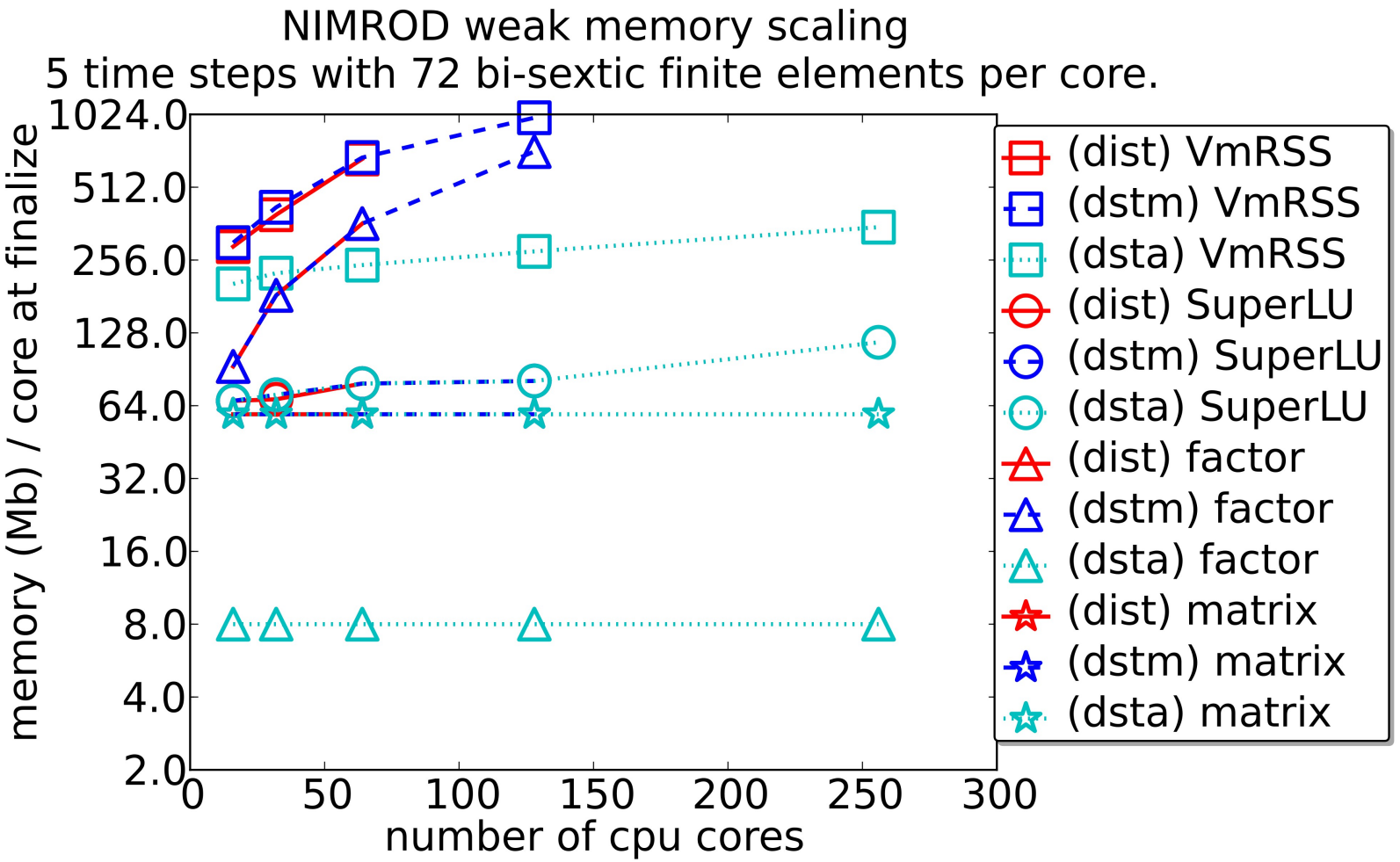

The ideal-like spectrum computed by NIMROD is comparable to that computed by ELITE and M3DC-1.

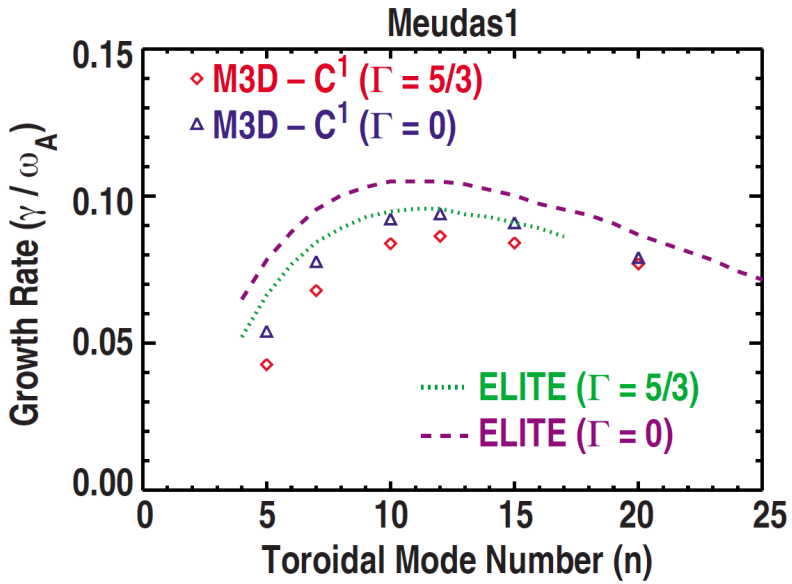

Meudas case
Ideal-like spectral convergence

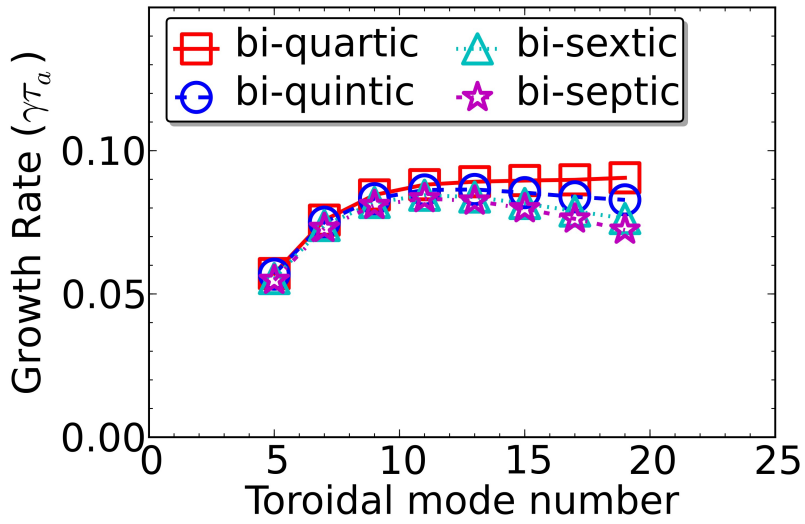

- The elimination of this memory-scaling bottleneck enabled a successful benchmark between ELITE and NIMROD on the 'Meudas' case, which was previously used as the basis of a benchmark between ELITE and M3D-C1 [1].
- In addition, we are now able to converge on cases that make use of NIMROD's extended-MHD model, which includes the use of anisotropic thermal conduction, ion gyroviscosity, and two-fluid and drift effects through the use of a generalized Ohm's law.

Upper left plot from Ferraro et al. (2010)
Meudas equilibria courtesy N Aiba

Convergence depends on resolving in a “diffraction pattern” from interference of inboard and outboard structure near the x-point.

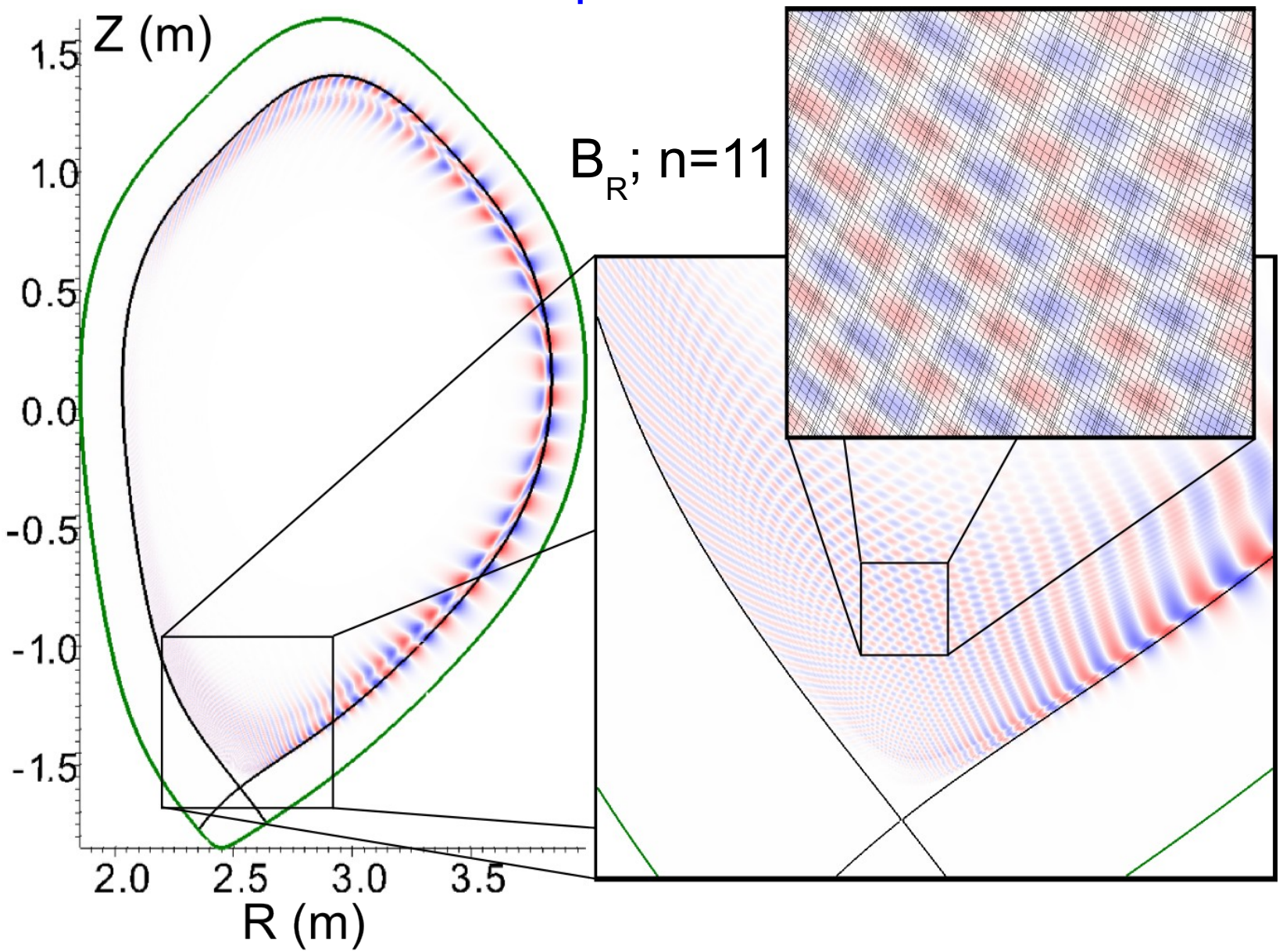

The DIII-D shot 14098 (left, t=4250 ms) reconstruction has a slightly steeper pedestal profiles than the Meudas benchmark case (right).

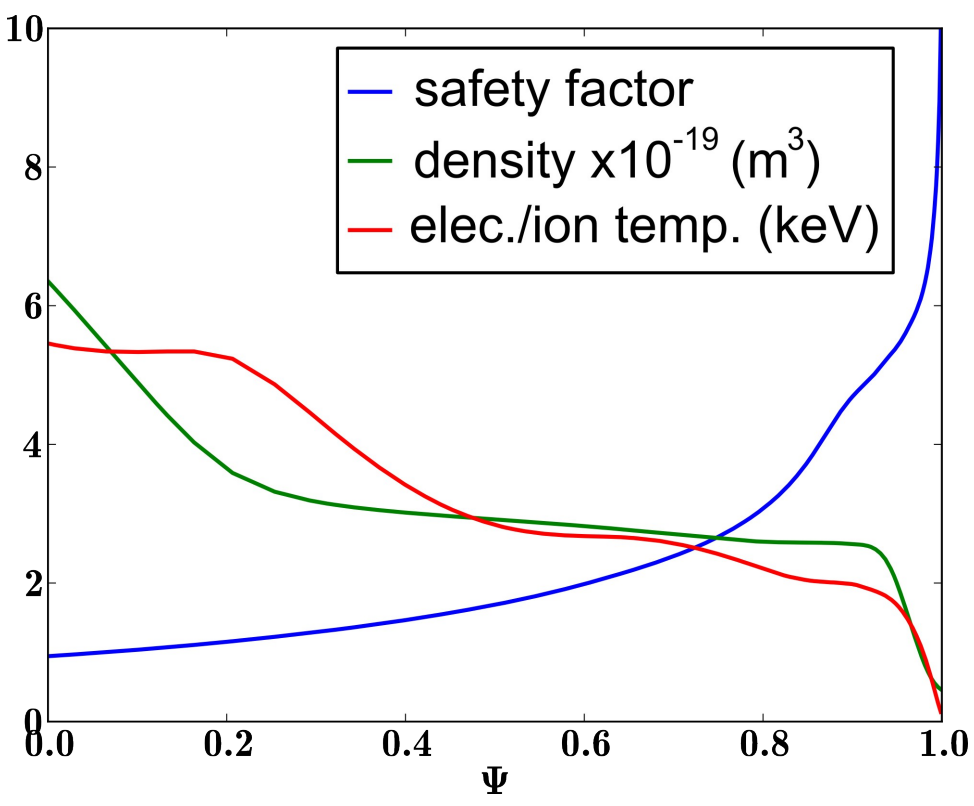

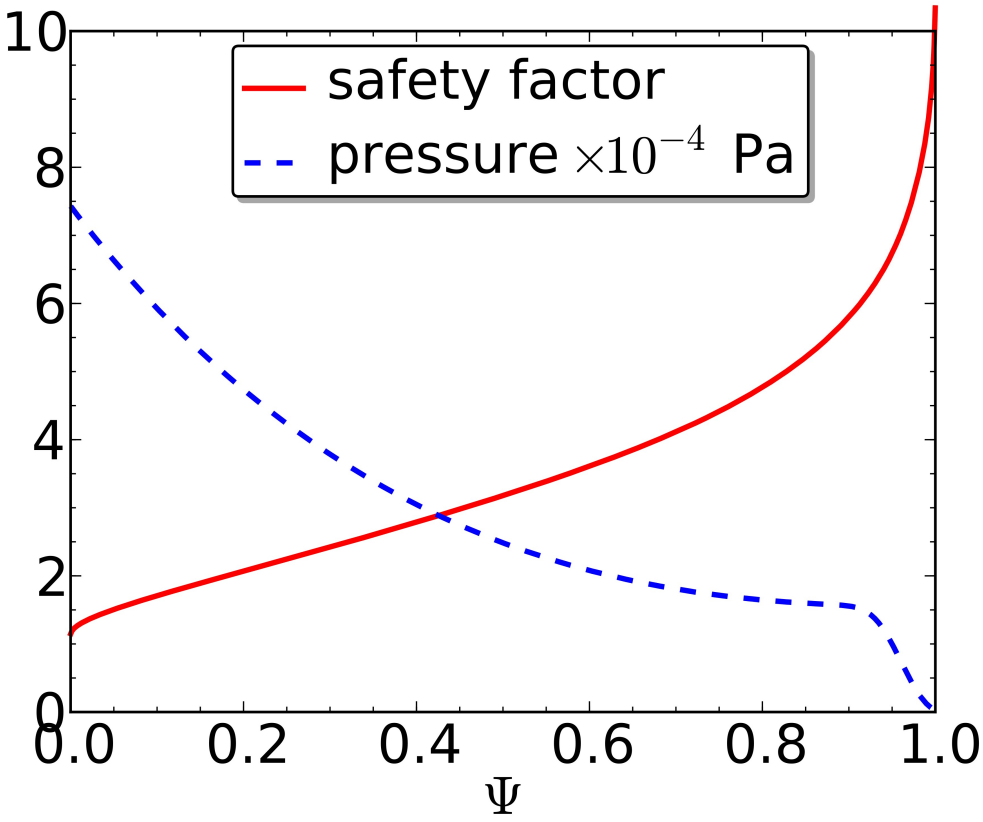

- The DIII-D case is also more strongly shaped with a more acute angle at the x-point.
- Equilibrium reconstruction courtesy Phil Snyder.

Running in the ideal-like limit to compare with ELITE requires step-function profiles for density and diffusivity.

- We have tried several approaches to get the ideal-like-limit cases running. In addition to using tanh functions to approximate step functions, we have also tried specifying the quadrature point values explicitly to avoid overshoots.
- Even without quadrature point overshoots, the FE weak form as implemented in NIMROD is not be amenable to discontinuous functions. Consider the RHS of the continuity equation where two regions are separated by the discontinuity in density:

$$-\int dV_p \alpha \nabla \cdot (n_p \mathbf{v}) - \int dV_v \alpha \nabla \cdot (n_v \mathbf{v})$$
$$= \int dV_p \nabla \alpha \cdot \mathbf{v} n_p + \int dV_v \nabla \alpha \cdot \mathbf{v} n_v$$
$$- \int dS_{pv} \cdot \mathbf{v} n_p \alpha - \int dS_{vp} \cdot \mathbf{v} n_v \alpha - \int dS_w \cdot \mathbf{v} n_v \alpha$$

- The surface terms at the plasma-vacuum interface do not cancel and are missing in our formulation.

Resistive-MHD cases converge from the stable side with the v-stabilization methods.

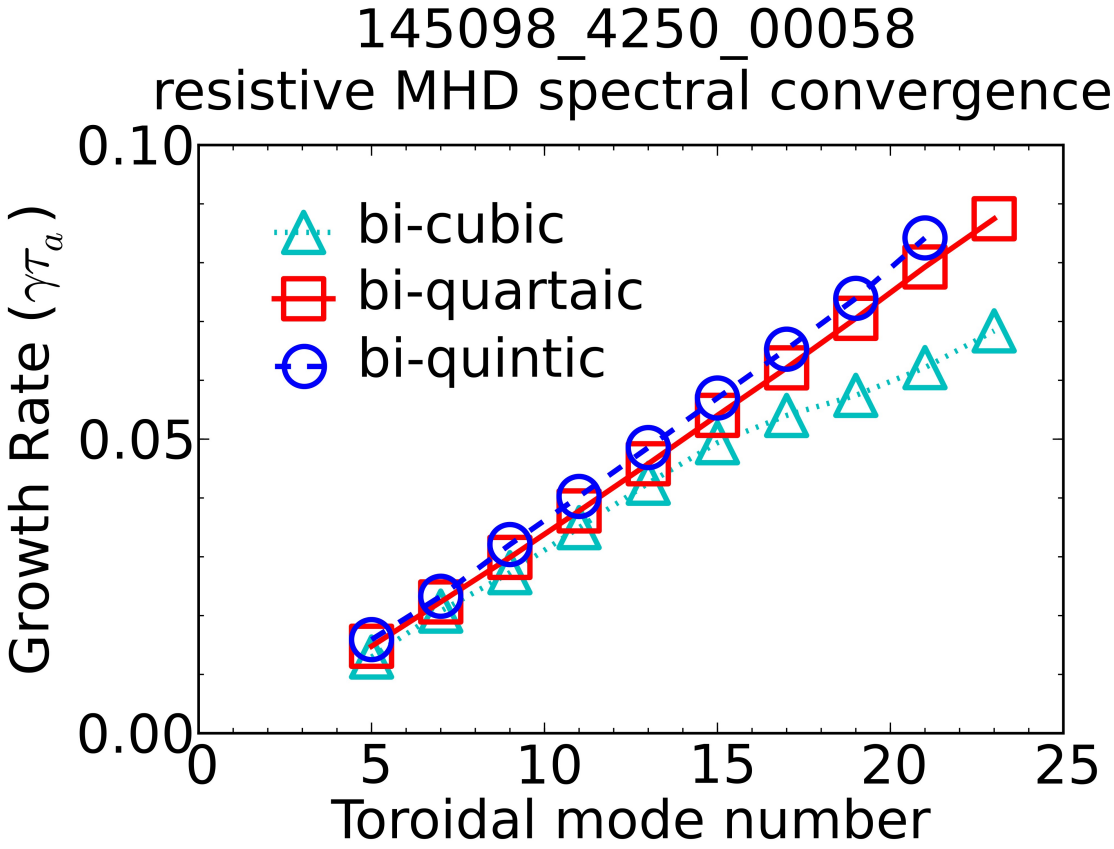

- These cases use reconstructed density and Spitzer-resistivity profiles with Ti=Te=50 eV at the separatix.
- The spectrum is more ballooning-like than the n=11 peaked spectrum computed by ELITE (with step-function density and resistivity profiles and an ideal-MHD model)

The pressure mode-structure is reasonably well converged and highly localized.

Pressure contours

n=5

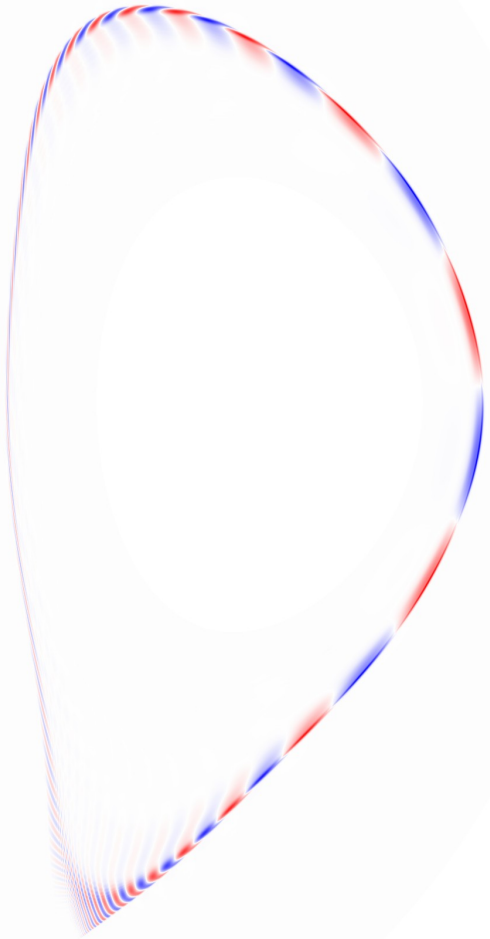

n=11

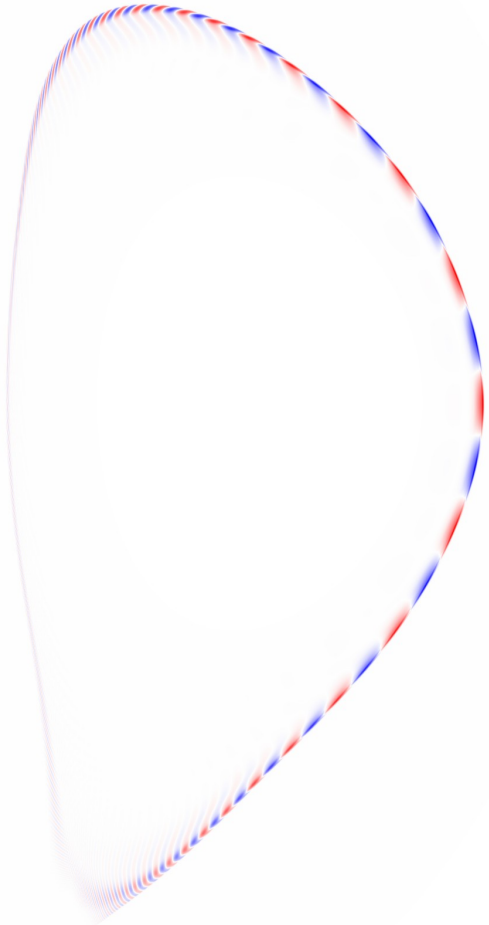

n=21

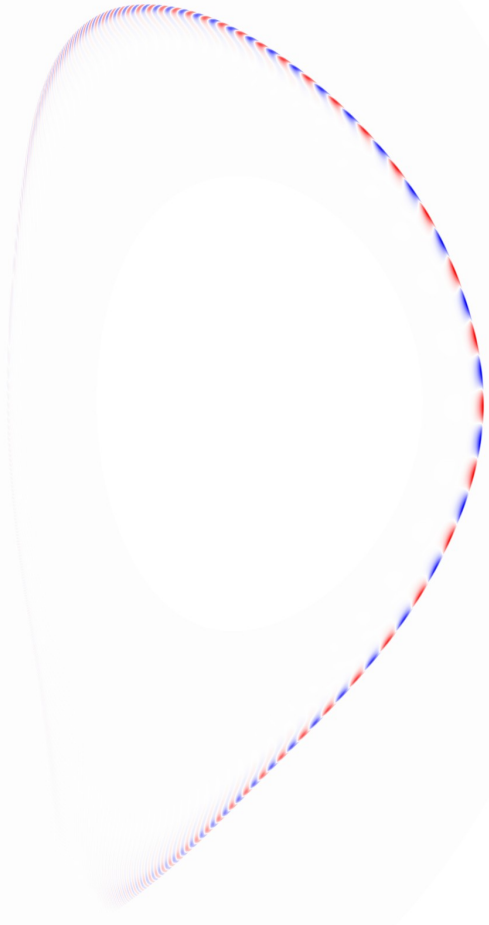

The magnetic mode-structure becomes localized at higher toroidal-mode numbers.

BR contours

n=5

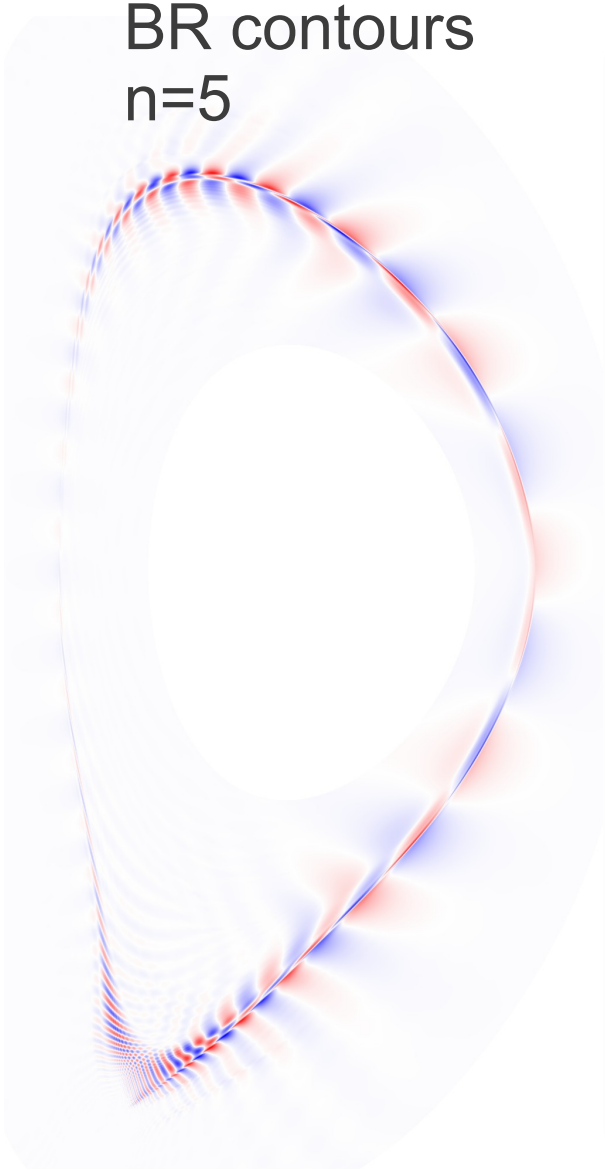

n=11

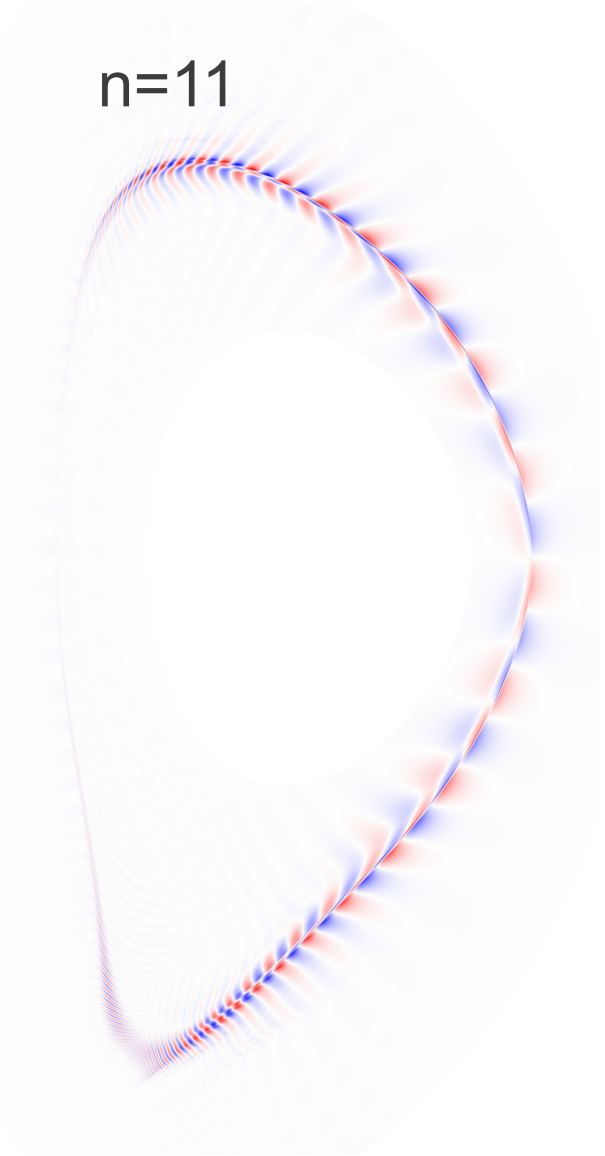

n=21

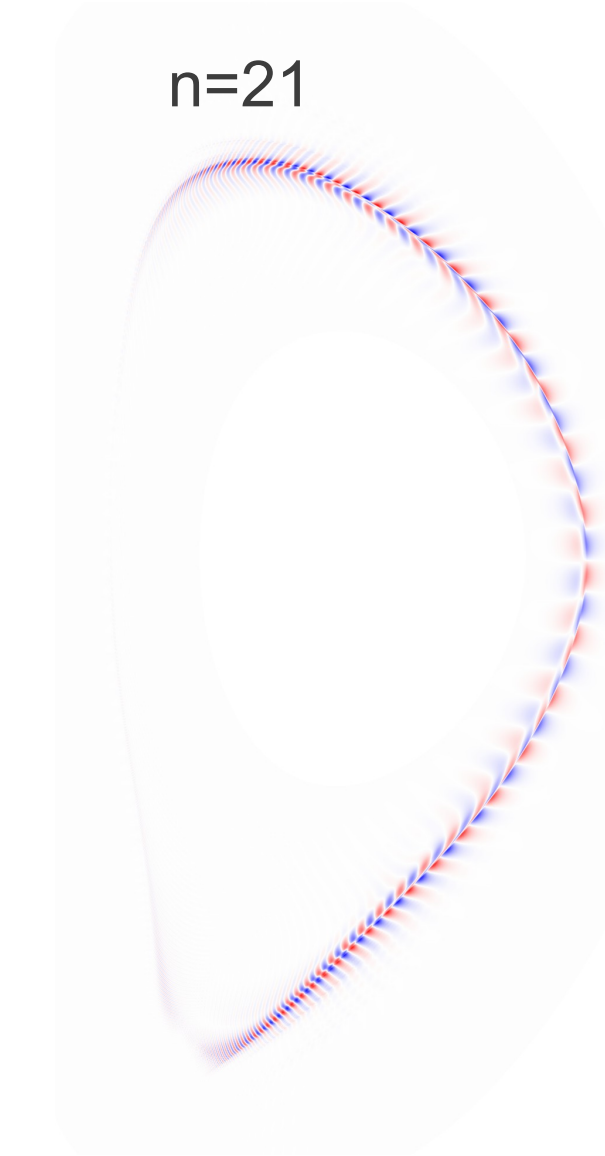

The velocity mode-structure is highly localized at all toroidal-mode numbers (Pm=1).

VR contours

n=5

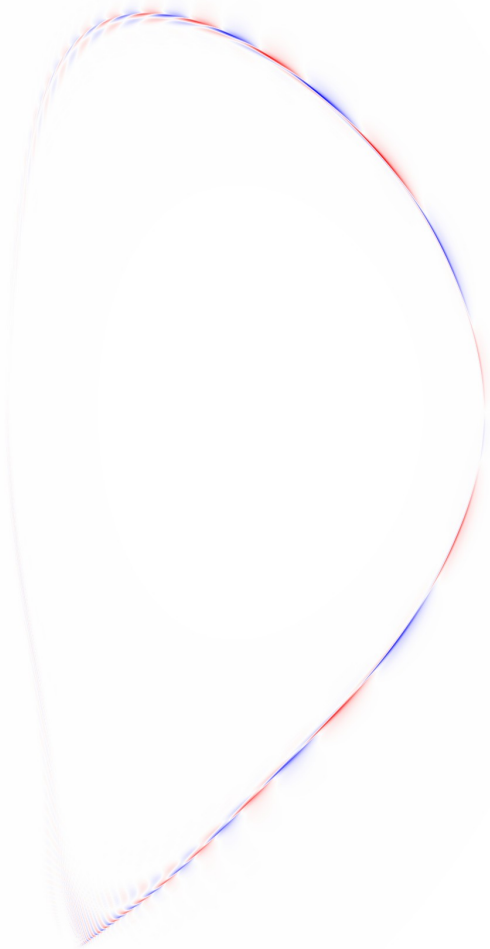

n=11

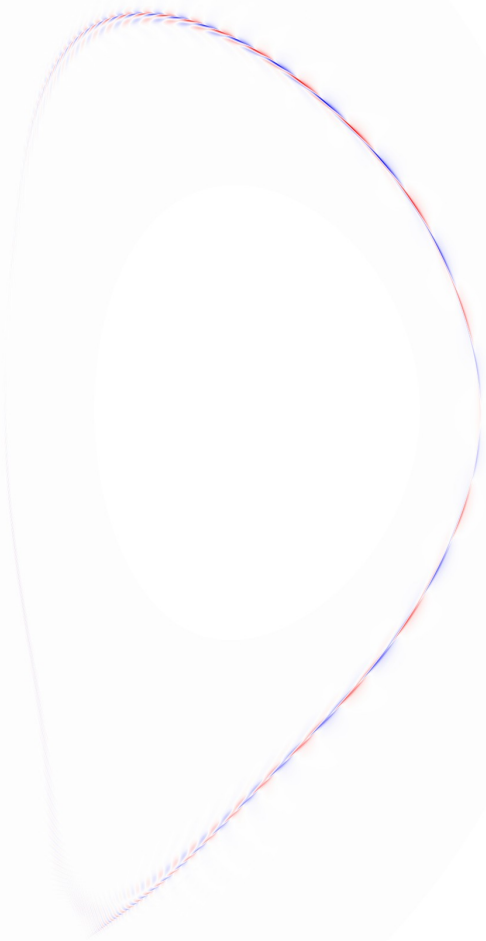

n=21

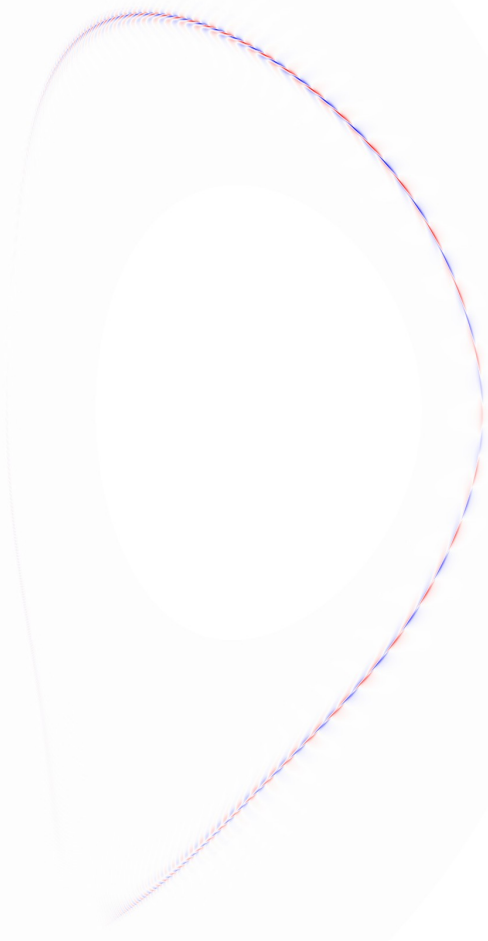

Going forward we intend to focus on modeling cases with flow and nonlinear dynamics.

$$\mathbf{v}_{EQ} = f_p K_p(\psi)\,\mathbf{B} + f_{E\times B}\Omega_{E\times B} R\hat{\phi} - f_{\nabla p}\Omega_{\nabla p} R\hat{\phi}$$

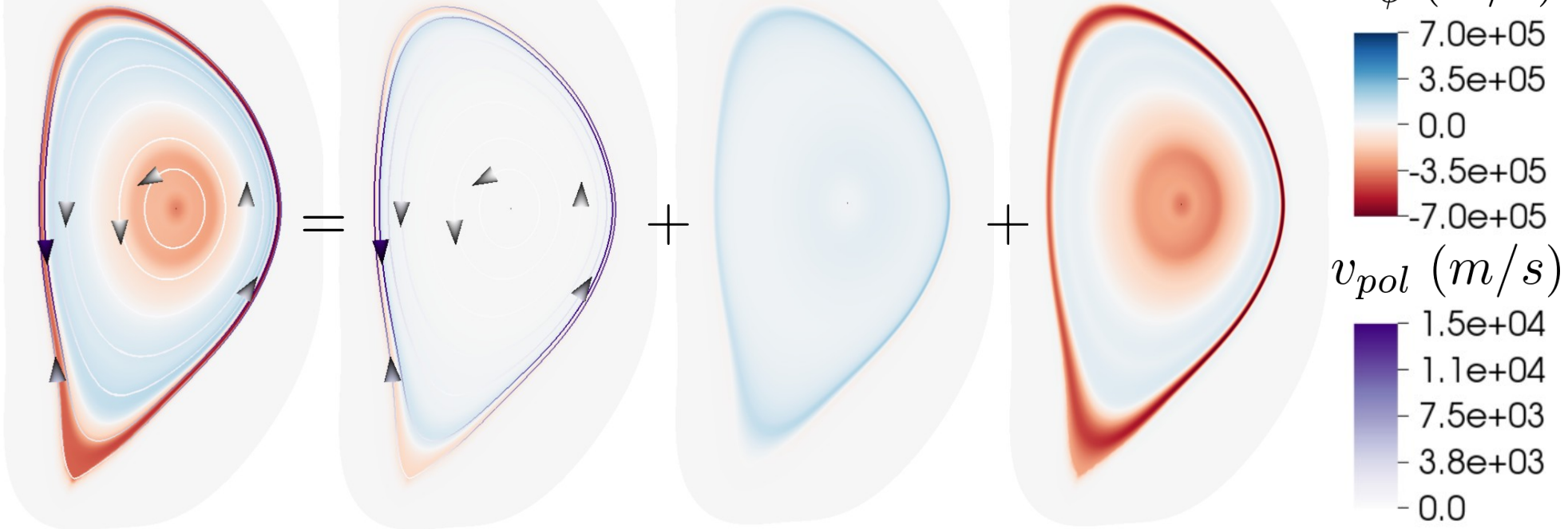

- We can vary the each contributions flow profiles, here we run cases with and without the ExB flow contribution.
- Profiles are shown for $f_p = f_{E\times B} = f_{\nabla p} = 1$.
- Flows are specified by the reconstruction up to the separatrix and extrapolated to zero beyond the separatrix. The extrapolation methods are a work in progress.

Summary

- We have made improvements to the NIMROD code that enable previously unachievable simulations.
- With these improvements, we can successfully benchmarked the diverted, high-q_{95} 'meudas' case with ELITE..
- We are able to run linear, resistive-MHD, high-q_{95} cases on DIII-D with edge harmonic oscillations (EHO).

Discussion

- There remains a qualitative discrepancy between the ELITE and NIMROD growth-rate spectrums.
- Future work will prioritize computations with flow and investigations of the nonlinear dynamics (Ideally, these will investigate saturation of the mode with dominant low-n harmonics)

Additional Slides

Comparison of the ELITE ideal-like results with the NIMROD resistive-MHD model (with full density and Spitzer-resistivity profiles).

ELITE

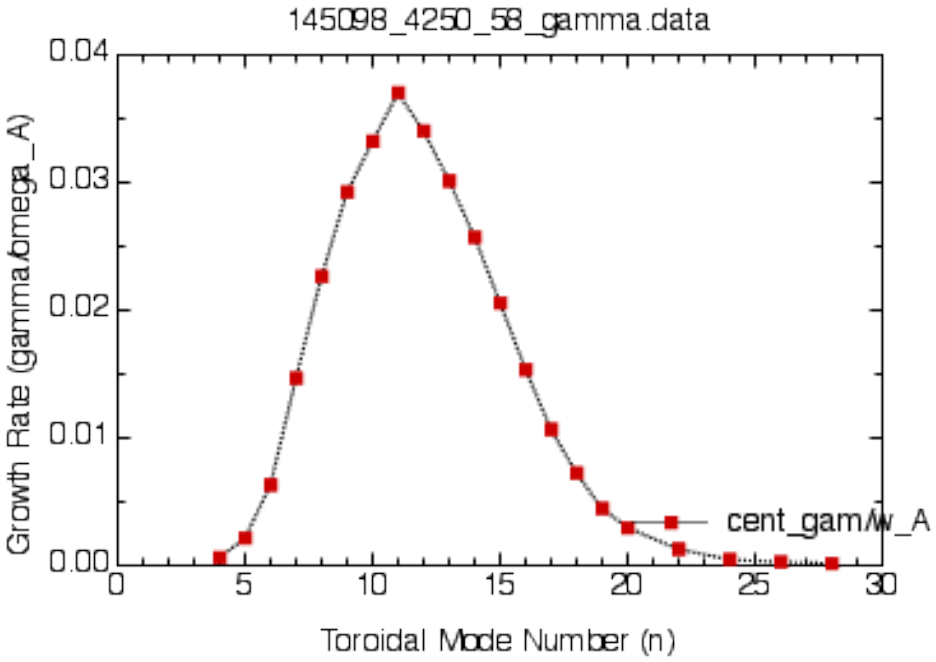

NIMROD

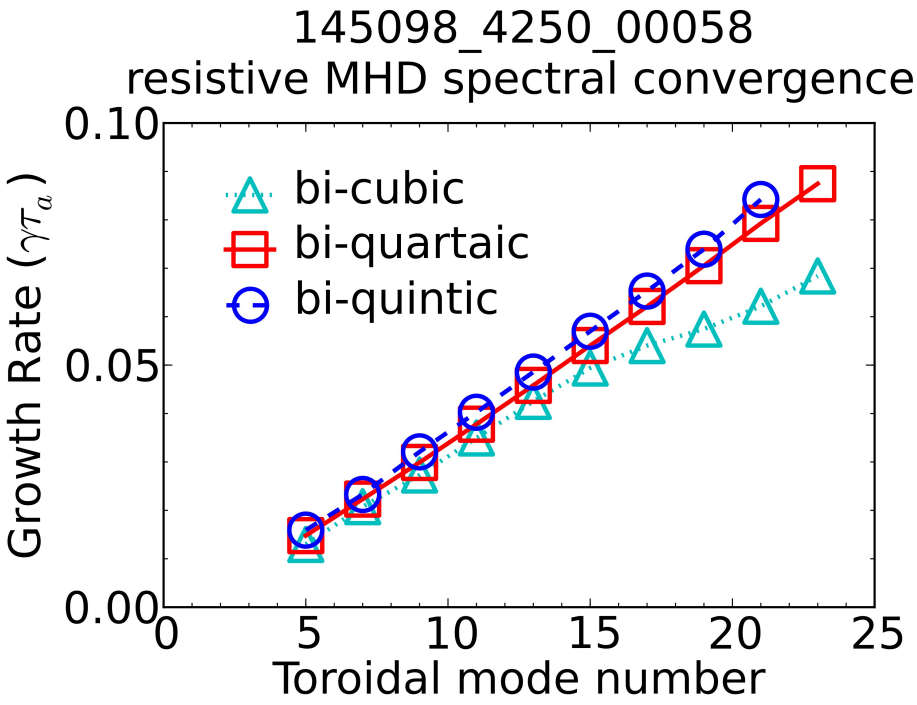

We analyze DIII-D shot 145098 at 4250 ms while the discharge is ELM free with broadband EHO.

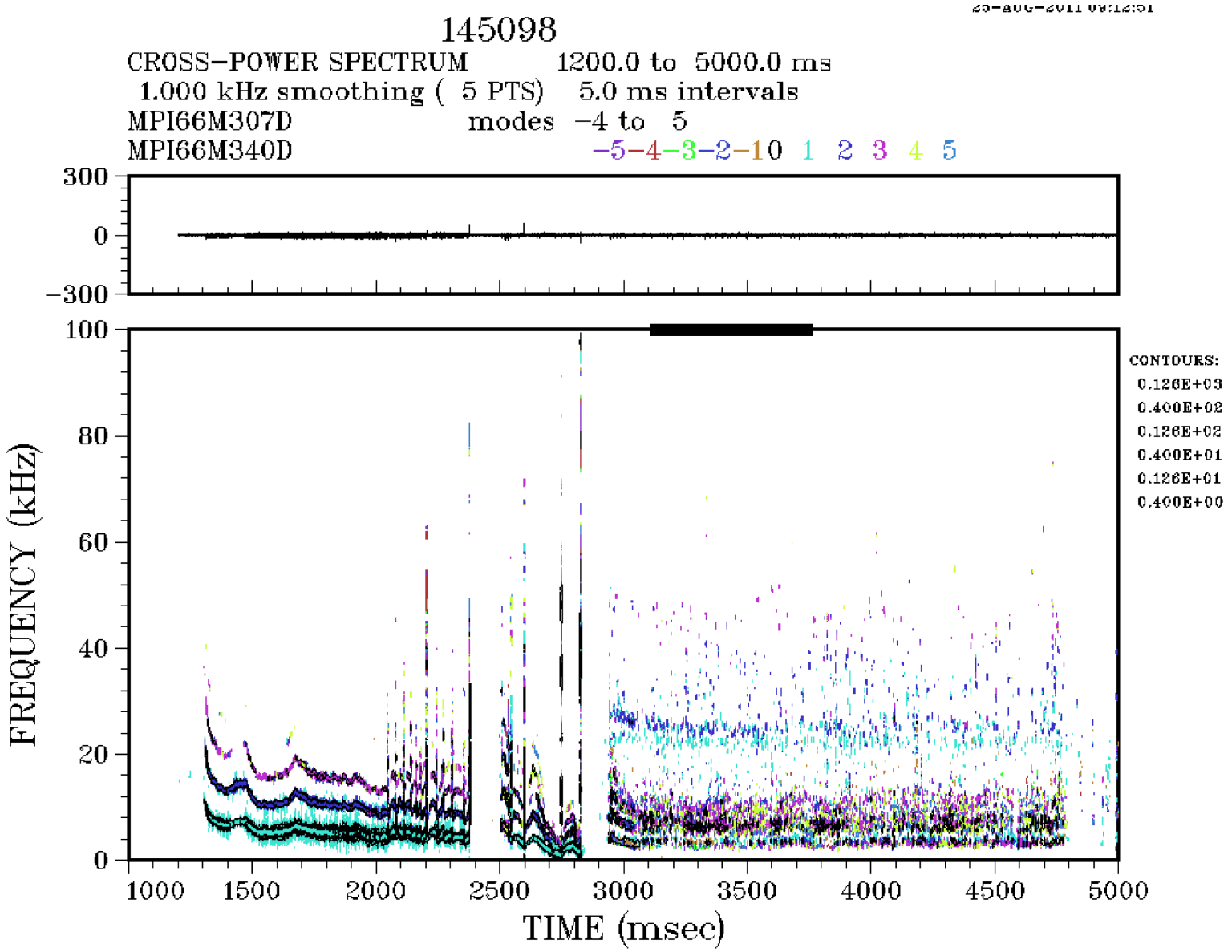

DIII-D discharge 145098 (right, designed to mimic ITER shaping) is more strongly shaped than the JT60-U Meudas benchmark case (left).

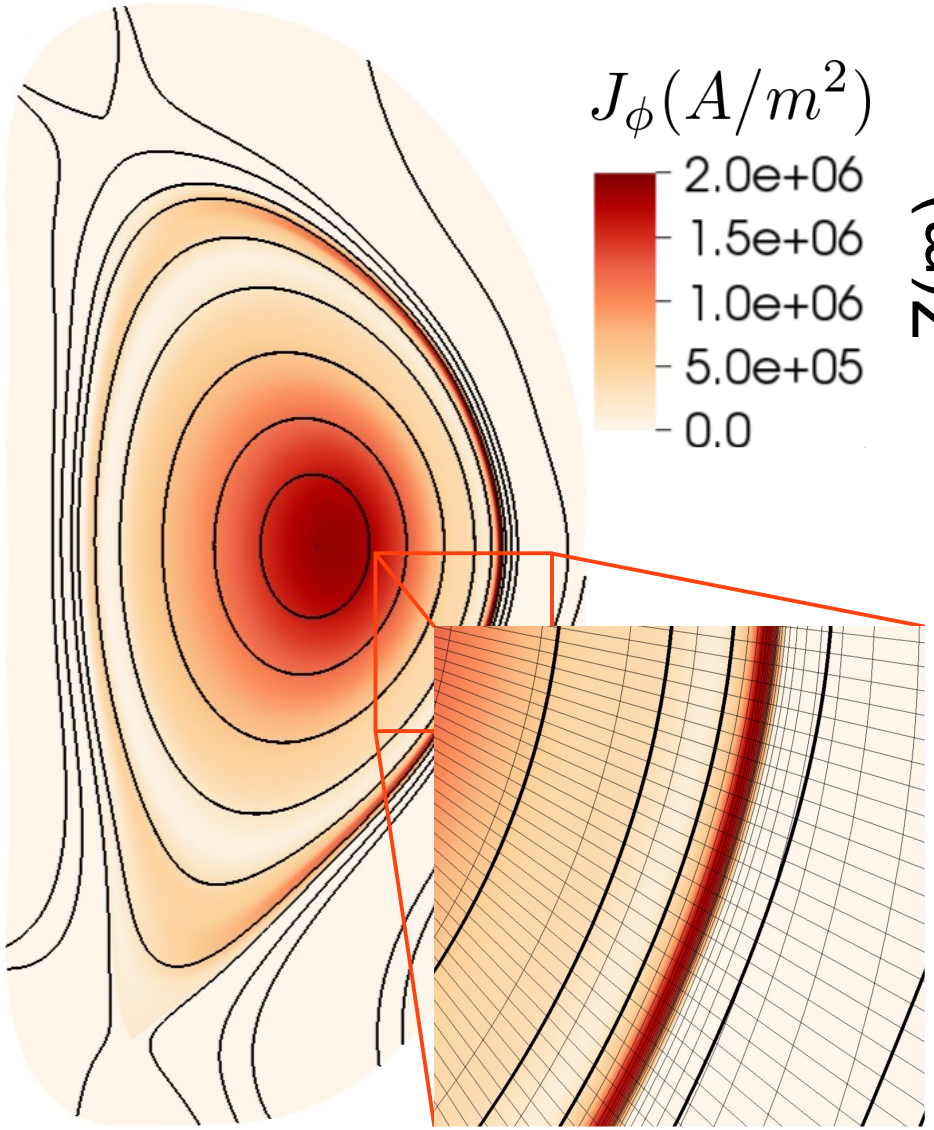

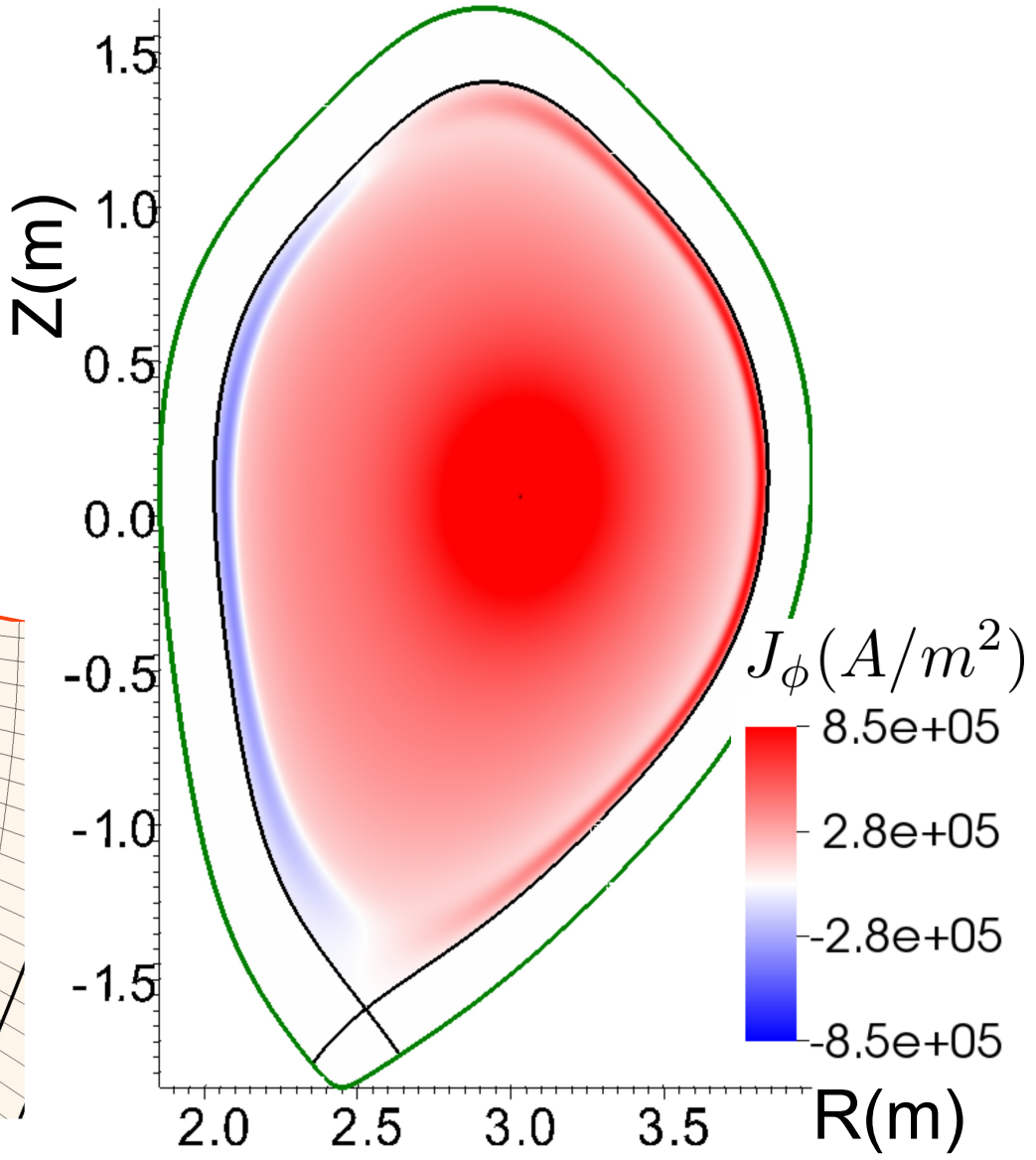

TECH-X

Our model captures flow-shear, parallel-physics, finite-Larmor-radius, and two-fluid effects.

$$\frac{\partial n}{\partial t} + \mathbf{v}\cdot\nabla n = -n\nabla\cdot\mathbf{v} + D_n\nabla^2 n$$

$$m_i n\frac{\partial \mathbf{v}}{\partial t} + m_i n\mathbf{v}\cdot\nabla\mathbf{v} = \mathbf{J}\times\mathbf{B} - \nabla p - \nabla\cdot\mathbf{\Pi} - \nabla\cdot\nu m_i n\mathbf{W}$$

$$\frac{n}{\Gamma-1}\left(\frac{\partial T}{\partial t} + \mathbf{v}\cdot\nabla T\right) = -nT\nabla\cdot\mathbf{v} + \nabla\cdot\left(n\chi_{\parallel}\hat{\mathbf{b}}\hat{\mathbf{b}}\cdot\nabla T\right)$$

$$\mathbf{\Pi} = \frac{m_\alpha p_\alpha}{4eB}\left[\hat{\mathbf{b}}\times\mathbf{W}_\alpha\cdot\left(\mathbf{I}+3\hat{\mathbf{b}}\hat{\mathbf{b}}\right) - \left(\mathbf{I}+3\hat{\mathbf{b}}\hat{\mathbf{b}}\right)\cdot\mathbf{W}_\alpha\times\hat{\mathbf{b}}\right]$$

$$+\nu_{\parallel}m_i n\left(\hat{\mathbf{b}}\hat{\mathbf{b}} - \frac{1}{3}\mathbf{I}\right)\left(3\hat{\mathbf{b}}\cdot\nabla\mathbf{v}_\alpha\cdot\hat{\mathbf{b}} - \nabla\cdot\mathbf{v}_\alpha\right)$$

$$\mathbf{E} = -\mathbf{v}\times\mathbf{B} + \frac{\mathbf{J}\times\mathbf{B}}{ne} - \frac{\nabla p_e}{ne} + \eta\mathbf{J} - \frac{m_e}{e}\frac{\partial\mathbf{v}_e}{\partial t}$$

$$\frac{\partial\mathbf{B}}{\partial t} = -\nabla\times\mathbf{E} \qquad \mathbf{J} = \nabla\times\mathbf{B} \qquad p_\alpha = nT_\alpha$$

The new distributed sparsity pattern interface (dsta) is at least as fast as the previous implementations.

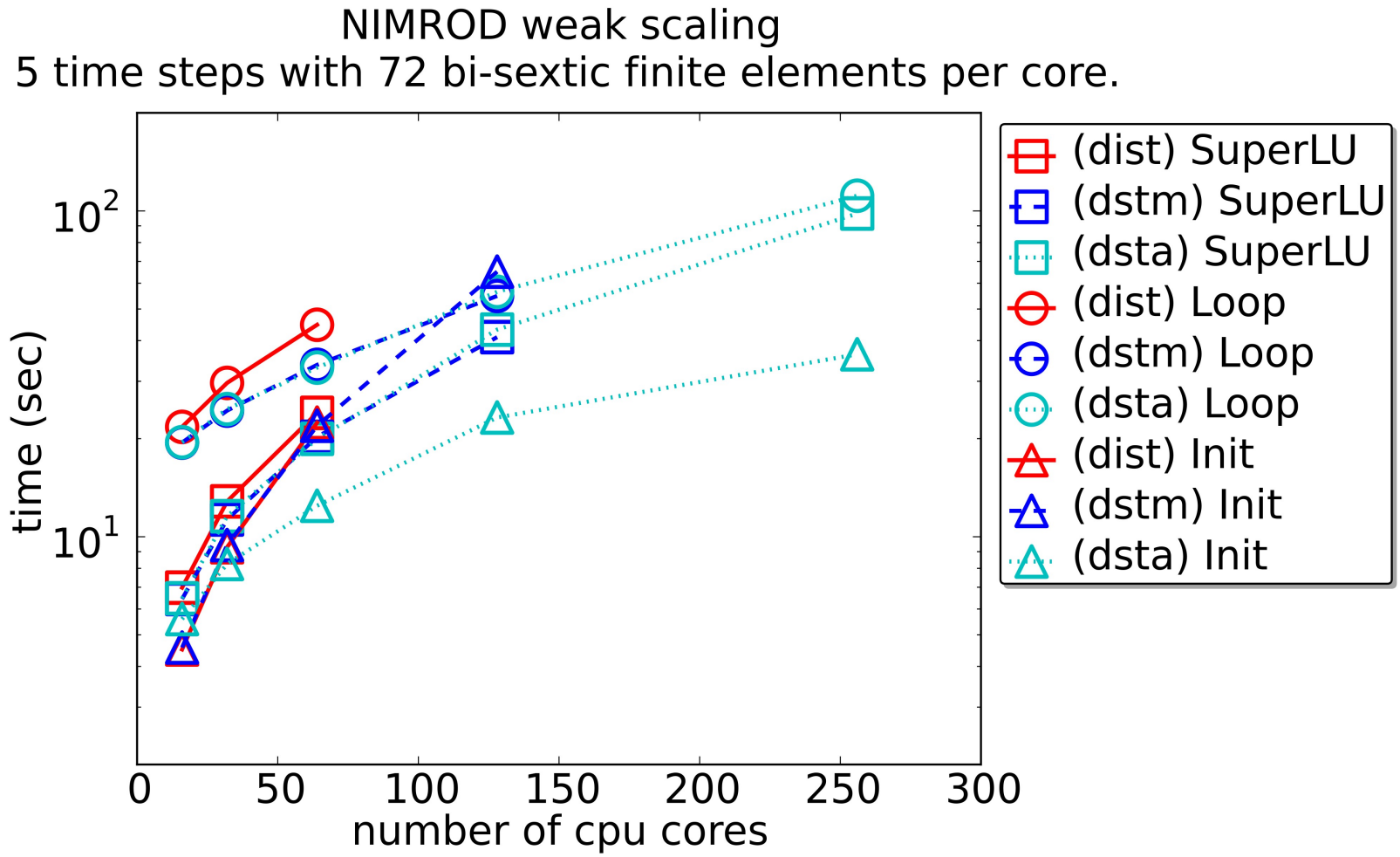

This example case uses SuperLU to obtain the LU factor decomposition and solves for only five time steps. Typical linear-physics cases require thousands of time steps without matrix factorization, thus the time-to-solution scaling shown here is for comparison only and not characteristic of a typical use case.

The eigenmode is qualitatively similar to that seen by M3D-C1, although the NIMROD wall location differs.

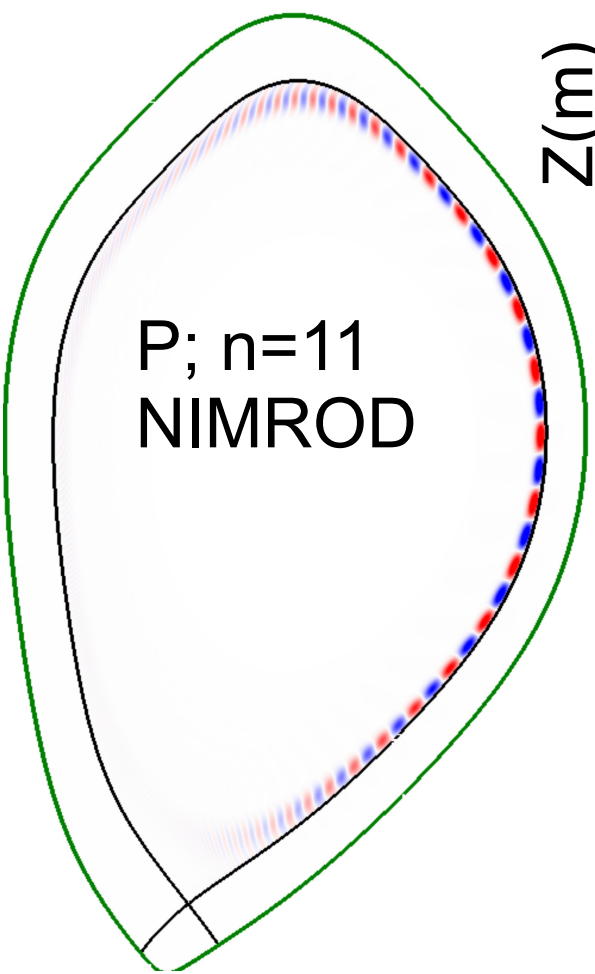

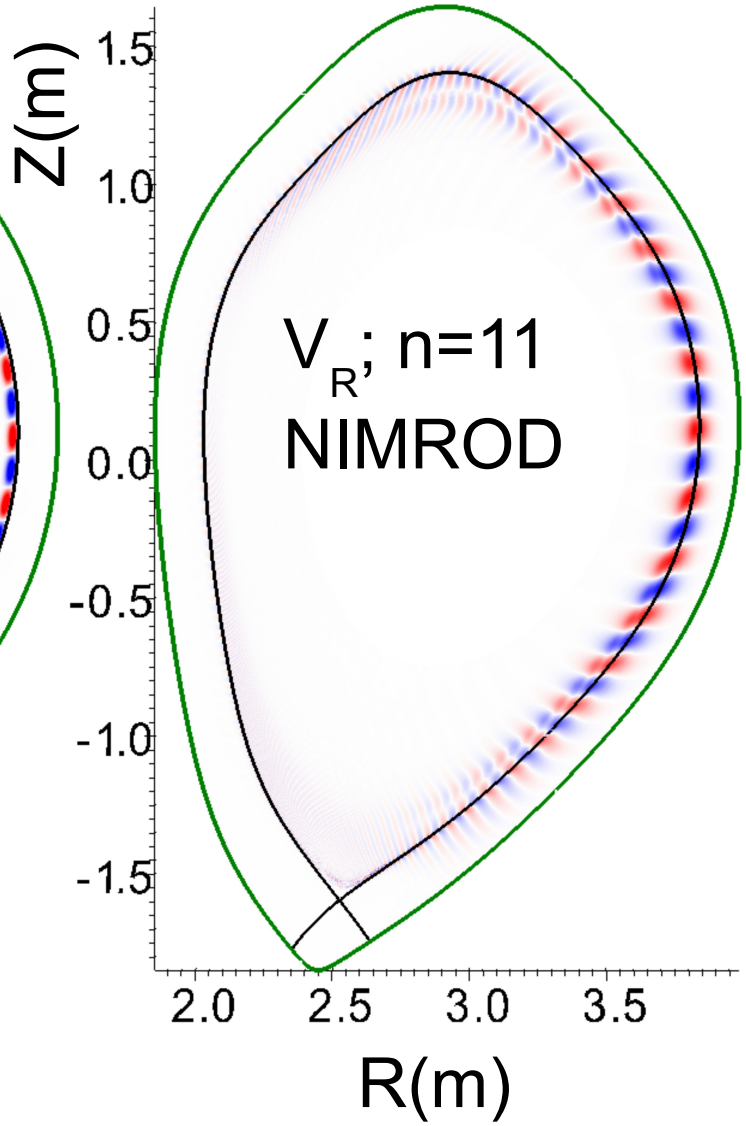

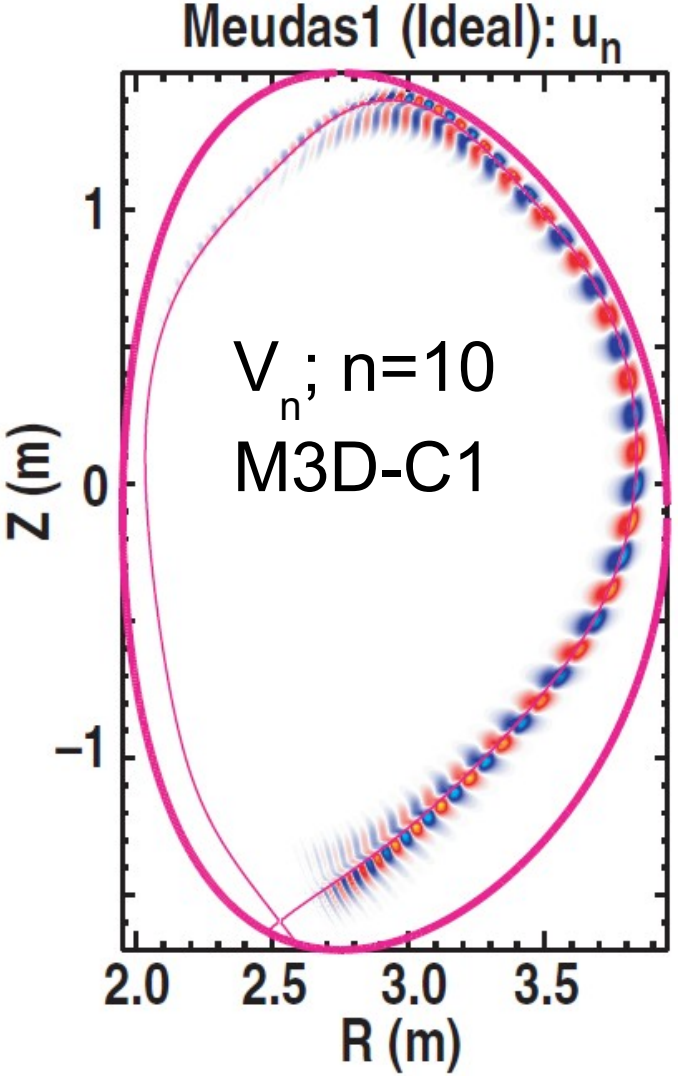

Ferraro et al. (2010)